Water-carbon dioxide mixtures at high temperatures and pressures as studied by infrared and Raman spectroscopies

Thierry Tassaing[1*], R. Oparin[2], Y. Danten[1] and Marcel Besnard[1]

[1]Laboratoire de Physico-Chimie Moléculaire, CNRS (UMR 5803),
Université de Bordeaux I, 351 Cours de la Libération, 33405 Talence Cedex, France.
[*]E-mail: t.tassaing@lpcm.u-bordeaux1.fr
[2]Institute of Solution Chemistry of Russian Academy of Sciences,
1, Akademicheskaya st., 153045 Ivanovo, Russia.

The state of aggregation of water dissolved in supercritical carbon dioxide has been investigated under isobaric heating (T=40-340°C, P=250 bar) using infrared absorption and Raman scattering spectroscopies. Quantitative analysis of experimental spectra has shown that below 100°C, water exists only in its monomeric form (solitary water surrounded by CO_2 molecules) whereas H-bonded species, namely dimers, begin to appear at higher temperature. At the same time, the ratio of dimers to monomers concentration increases with further temperature increase and at temperatures close to the temperature of total miscibility of the mixture (T=366°C, P=250 bar), only water dimers are present in the CO_2-rich phase.

1. Introduction

The geochemical and technological importance of the water-carbon dioxide system is profound, particularly for protection of the environment where new industrial processes for water purification and waste destruction are developed [1]. In these research areas, fundamental knowledge about the reactivity between organic/mineral species and water and CO_2 are needed in order to understand the various mechanisms involved in these processes. In this context, the binary system H_2O-CO_2 has been the subject of numerous experimental [2,3] and theoretical [4,5] thermodynamics to investigate phase diagrams, mutual solubilities and densities as a function of temperature and pressure. In particular, the solubility of water in carbon dioxide, which is very low at ambient conditions ($\approx 10^{-2}$ molar fraction), increases strongly with temperature to reach a complete miscibility at temperature around or slightly below the critical temperature of water. Let's emphasise that the temperature of total miscibility of CO_2 and water is strongly dependent upon the pressure and found to be minimum at 266°C for P=2500 bar. In this study, we have chosen to work at a constant pressure of 250 bar at which the total miscibility is reached at T=366°C [2]. The choice of these conditions was guided by the fact that it is necessary to be above the critical pressure of pure water ($P_c(H_2O)$=220 bar) to access at a given temperature to a complete miscibility of the two constituent leading to a homogeneous phase. Below the critical pressure of water, we may have two phases (liquid and vapour) without obtaining a total miscibility at higher temperature. In addition, most of the industrial processes involving hydrothermal oxidation are performed at pressures ranging between 250-300 bar. Finally, these thermodynamic conditions exist at the bottom of ocean close to hydrothermal vents [6]. In this work, we want to get information at a microscopic level about the structure and dynamics of water dissolved in the CO_2 rich phase at constant pressure P=250 bar as a function of temperature in order to try to understand the solvation process in this medium. For this task, vibrational spectroscopic methods provide a powerful tool. In particular, the OH stretching band of water is very sensitive to the strength of the interaction between water and the surrounding solvent molecules [7]. Few works have been undertaken to study CO_2/water solutions under supercritical conditions. In the study by M.J Clarke et al. [8], although main part of the work was devoted to a study of the state of water aggregation in micro-emulsions, the spectrum of D_2O dissolved in CO_2 has been reported at 32°C and P=156 bar and it was concluded that water was almost free in supercritical carbon dioxide. Another study by L.E. Bowman et al. [9] has shown that the rotational

motion of water in CO_2 was hindered because of the dipole-quadrupole interactions between water and CO_2. The nature of the interaction existing between water and carbon dioxide has also been addressed on the basis of abinitio theoretical works [10,11]. A Lewis acid-base type of interaction has been put in evidence in which the CO_2 carbon atom and the oxygen atom of water play respectively the role of the electron acceptor and donor. It was shown that this interaction plays a role on the rotational dynamics of water in SC CO_2 [12]. In this context, we have performed a quantitative analysis of the infrared absorption spectra of deuterated water highly diluted in supercritical CO_2 using an analytical model to assess the contribution of repulsive and attractive forces between the water and CO_2 molecules and to evaluate the weight of the different terms (namely, dispersion, induction and dipole-quadrupole forces) in the interaction energy and shifts [13]. Under thermodynamic conditions close to ours, the water-CO_2 mixtures have been investigated by N.M.R. spectroscopy to measure the translational diffusion coefficient of water in supercritical carbon dioxide [14]. To the best of our knowledge, all these spectroscopic studies have been limited in the low concentration/temperature range.

The aim of the present paper is to provide a vibrational spectroscopic study of the evolution of the structure of water diluted in supercritical carbon dioxide as a function of temperature and at constant pressure. In the first part, we will present the near infrared spectra (4500-7500 cm^{-1}) of H_2O diluted in supercritical carbon dioxide at constant pressure p=250 bar and high temperatures (40-360°C). Then the Raman spectra of H_2O diluted in supercritical CO_2 under the same conditions will be presented. The third part of this article will be devoted to the presentation of the mid infrared investigation on HOD diluted in supercritical carbon dioxide under the same thermodynamic conditions. Finally, we will compare the Raman and mid-infrared results to give a consistent picture of the distribution of the various species existing in the fluid.

2. Experimental Methods

For Raman scattering and infrared absorption experiments the same stainless steel cell [15] has been used. It was equipped with two cylindrical windows (silica for Raman and sapphire for IR) with a pathlength of 4.5 mm. The sealing was obtained using the unsupported area principle. The windows were positioned on the flat surface of inconel plug with a golden foil placed between the windows and the plug in order to compensate for imperfections at the two surfaces. Flat graphite rings were used to ensure sealing between the plug and the cell body. The heating was achieved using four cartridge heaters disposed in the body of the cell. To control the temperature, two thermocouples were used. The first one was located close to one cartridge in order to achieve a good temperature regulation. The second one, close to the sample area, allowed to measure the temperature of the mixture with an accuracy of about $\Delta T = \pm 0.5$°C. The cell was connected via a stainless capillary tube to a hydraulic pressuring system which allows to attain pressure up to 500 bar with an absolute uncertainty of ±1 bar and relative error ±0.3%.

The lower part of the cell was partially filled with water in order to get its level slightly below the incoming beam and CO_2 (purchased from Air Liquid (99.995% purity)) was added and used as the pressurizing fluid. Ultra pure water (milli Q, 18 M Ω.cm)) and D_2O (99.9% purity, purchased from CEA Saclay, France) were used.

In the mid IR region, the OH stretching region of water cannot be observed due to the strong absorption of combination modes ($2\nu_2+\nu_3$ and $\nu_1+\nu_3$) of CO_2 existing in the same spectral domain. Moreover, measurement of the IR spectra of pure D_2O is precluded due to the need of using a short pathlength of about 100 μm (for the highest water concentration) which might lead to bad equilibration of the water/CO_2 mixture due to capillarity effects between windows. Therefore, isotopic water mixture of D_2O and H_2O with ratio of 1:20 has been used leading to D_2O, HDO and H_2O species with the following approximate proportion 1:40:400 respectively at ambient conditions. For this "isotopic" mixture, the infrared absorption in the OD stretching region (2500-2900 cm^{-1}) can be assigned only to HDO with a good approximation. Although we were unable to get the IR spectrum in the OH stretching region of water, it was possible to measure in the near infrared region (4500-7500 cm^{-1}) the combination modes and the overtones of H_2O and CO_2 with a good accuracy.

The infrared absorption measurements were performed on a Biorad interferometer (type FTS-60A) equipped with a globar source, a KBr beam splitter and a DTGS detector. Single beam spectra recorded in the spectral range 400-7500 cm^{-1} with a 2 cm^{-1} resolution were obtained after

Fourier transformation of 50 accumulated interferograms. Double beam spectra were calculated by ratioing the single beam spectra of the sample by the background. Absorbance spectra of water in the binary mixtures were obtained after subtracting the neat CO_2 spectra measured under the same thermodynamic conditions.

The Raman spectra were collected on a DILOR Labram confocal spectrograph equipped with a CCD detector. The source was a Spectra Physics argon-krypton laser operating at a wavelength of 514.5 nm with a power of 300 mW. The polarized I_{VV} and depolarized I_{VH} spectra were recorded using a back scattering geometry with 3 cm^{-1} resolution in the range 3400-3750 cm^{-1}. Baseline corrections were performed on the spectra to remove a small background contribution. We always found that the depolarized $I_{VH}(\bar{\nu})$ spectra are extremely weak compared to the polarized ones and will not be discussed further here.

3. Thermodynamics details

The phase diagram of the binary mixture H_2O-CO_2 drawn from Todheide's thermodynamics data [2] is displayed on Figure 1 and gives the evolution with the temperature of the mutual solubility of water and carbon dioxide at constant pressure P=250 bar. Clearly, the solubility of H_2O in CO_2 which is very low at ambient condition (below 10 % mol. in the temperature range 40 to 180°C) strongly increases upon heating to reach a total miscibility at 366°C. Using the thermodynamic data reported in the literature [2], we have estimated for the binary system the evolution of the water concentration C_{H2O} in the CO_2 rich phase as a function of the temperature corresponding to the molar fraction x_{H2O} (mol of water per 100 mol of solution). The values C_{H2O} have been calculated

$$C_{H_2O} = \frac{\rho}{M_{H_2O} + M_{CO2}(1/x_{H2O} - 1)}$$

and are reported in insert of figure 1. The density ρ of the CO_2 rich phase (see insert of figure 1) was obtained using an equation of state which reproduces nicely the experimental phase diagram of the binary mixture H_2O-CO_2 [5]. In the next part of this paper, we will also estimate the evolution of the concentration of water in CO_2 as a function of temperature from the intensity variation of a combination mode and an overtone of H_2O in order to compare with the thermodynamics measurements.

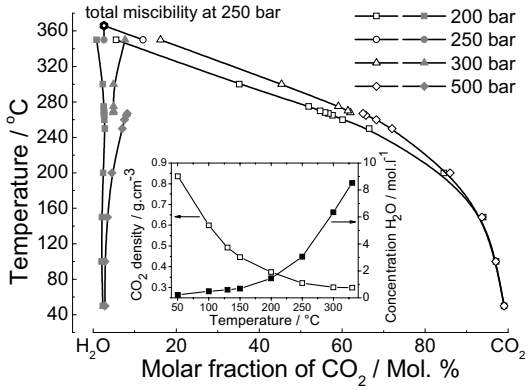

Fig. 1: Phase diagram of the H_2O/CO_2 mixture at constant pressure. Insert: Concentration of water dissolved in CO_2 and density of the CO_2 rich phase as a function of the temperature at constant pressure P=250 bar.

4. Results

4.1. Near infrared region

We have reported in Figure 2 the near infrared spectra of the CO_2 rich phase of the H_2O-CO_2 mixtures recorded in the temperature range 40-340°C at constant pressure 250 bar without subtracting the CO_2 contribution. In the spectral range 4500-6000 cm^{-1}, we observe three narrow peaks centred at about 4840, 4960, 5100 cm^{-1} whose intensity decreases strongly upon the

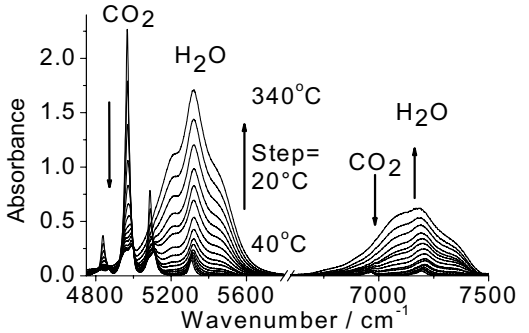

Fig. 2: Evolution with temperature at constant pressure P=250 bar of the near infrared spectra of the H_2O-CO_2 mixture.

increase of temperature which are respectively assigned to the combination modes $4\nu_2+\nu_3$, $\nu_1+2\nu_2+\nu_3$, $2\nu_1+\nu_3$ of the CO_2 molecule [16]. The small peak at about 5308 cm^{-1} which is enhanced

and broadened upon increasing temperature is associated with the combination mode $\nu_2+\nu_3$ of water [17]. Although the $\nu_2+\nu_1$ combination mode of water is active and should be detected around 5200 cm^{-1}, the dipole derivative associated with this transition is very small [17] and therefore the intensity of the associated spectrum is too weak to be detected. In the spectral range 6500-7500 cm^{-1}, the small peak at about 7195 cm^{-1} which is enhanced and broadened upon increasing temperature is associated with the overtone $2\nu_3$ of water [17]. The small peak observed at about 6955 cm^{-1} whose intensity decreases strongly upon the increase of temperature is assigned to the overtone $3\nu_3$ [16] of CO_2. These absorption changes reveal the variation of the concentrations of water and CO_2 with temperature in the CO_2 rich phase as expected from the phase diagram reported for the binary system H_2O-CO_2 in Figure 1. Indeed, upon increasing temperature, we observe an increase of the concentration of water in the mixture and a decrease of the CO_2 concentration. In order to estimate the concentration of water from the observed integrated intensities, we need to know the molar absorption coefficient K(ν) of the mode of water. As a first approximation,

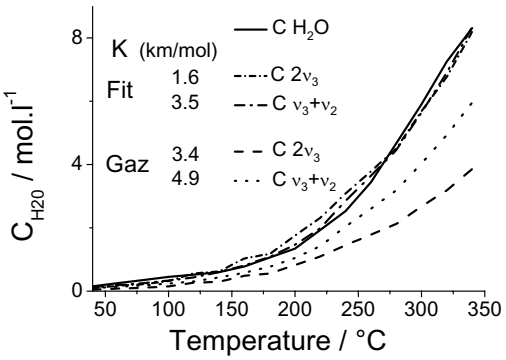

Fig. 3: Concentration of H_2O in the CO_2 rich phase for the mixture H_2O-CO_2 calculated from the integrated intensities of the NIR profiles associated with the combination mode $\nu_2+\nu_3$ and the overtone $2\nu_3$ of water (see text).

we have used the molar absorption coefficient K(ν) for water in the gas phase reported in the literature [17] for the combination mode $\nu_2+\nu_3$ (K(ν)= 4.83 $km.mol^{-1}$) and the overtone $2\nu_3$ of water (K(ν)= 3.38 $km.mol^{-1}$). The evolution of the concentration of water in CO_2 as a function of temperature extracted from the measured integrated intensities of $\nu_2+\nu_3$ and $2\nu_3$ is reported in Figure 3 and compared with the value reported by Todheide et al.[2]. The concentration extracted from the integrated areas of the two modes of water, significantly differ from each other and with the literature values. Although it is expected that combination modes and overtones of OH stretching modes are less sensitive to interactions (hydrogen bonding) and/or density effects with surrounding molecules than fundamental OH stretching modes [18], disagreements observed in Figure 3 mean that we can't make the hypothesis that the molar absorption coefficient of the $\nu_2+\nu_3$ and $2\nu_3$ modes is independent on the state of the water molecule. Moreover, it seems that the effect of the environment on the water molecule is different for the two modes. In this context, we have determined the molar absorption coefficients K(ν) of the $\nu_2+\nu_3$ and $2\nu_3$ mode of water that give an evolution of the concentration of water in agreement with the literature data. A good fit of the concentration data was obtained (see Figure 3) for K($\nu_2+\nu_3$)=3.5 $km.mol^{-1}$ and for K($2\nu_3$)=1.6 $km.mol^{-1}$. These values are in both cases smaller than that reported for water in the gas phase. This observation may be related to hydrogen bond complex formation in these water-CO_2 mixtures as it will be shown below. Indeed, it has been shown that the molar absorption coefficient of the OH group of the donor molecule in a water dimer is roughly half that of monomeric water [18]. Therefore, the decrease of the molar absorption coefficients of the $\nu_2+\nu_3$ and $2\nu_3$ modes compared to their respective gas phase values is consistent with the formation of water dimer in the water-CO_2 mixtures (see below). Finally, the good agreement obtained between our values and that reported by Todheide et al. indicates that proper equilibrium conditions were achieved in our study.

4.2. Raman spectroscopy

The polarized $I_{VV}(\bar{\nu})$ Raman spectra of the OH stretching mode of water in CO_2 measured from ambient temperature up to 340°C at constant pressure P=250 bar are displayed on Figure 4. Because scattering intensities are measured on an arbitrary scale, we have adopted the following procedure to allow a comparison of these spectra. We have assumed that the polarisability derivative involved in the spectral transition is independent of the state of aggregation of water and thus its integrated intensity is only proportional to the water concentration in the CO_2 phase. This approximation

which relies on the fact that the Raman activity of the OH stretching mode is not strongly dependent on hydrogen bonding [19] will be aposteriori justified.

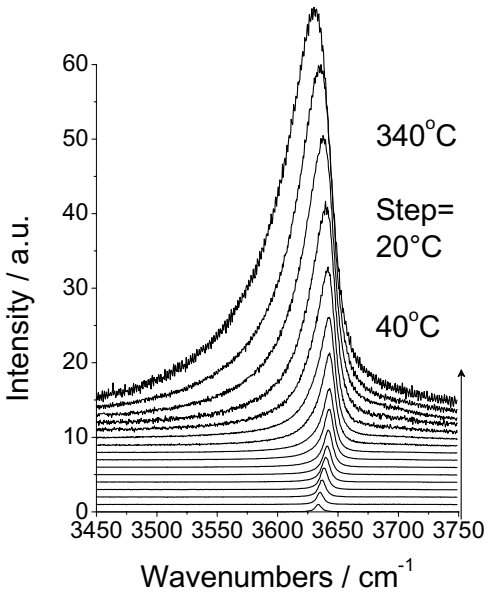

Fig. 4: Evolution of the Raman scattering spectra of H_2O in the CO_2 rich phase as a function of the temperature at constant pressure P=250 bar.

Thus, the spectra have been relatively normalized so that their integrated areas are proportional to the calculated water concentration in the CO_2 phase. In the low temperature range (40-80°C), we observe a well defined peak centered at about 3632 cm^{-1} which can be assigned to the symmetric stretching mode (ν_1) of H_2O monomer interacting with surrounding CO_2 molecules through an electron donor-acceptor interaction [10,12,13]. Although the ν_3 anti-symmetric stretch of water is active, the polarizability derivative associated with the corresponding transition is very small and therefore the intensity of the associated spectrum is too weak to be detected. Increasing the temperature, the band center of the previous profile shifts continuously towards higher frequencies to reach a maximum value of about 3644 cm^{-1} at T=180°C and then shifts to lower frequencies down to about 3630 cm^{-1} at the highest temperature investigated. Concurrently, the width of the profile which remains rather narrow (i.e. of about 8 cm^{-1}) up to T=200°C starts to strongly broaden leading to the observation of a very broad asymmetric profile at high temperature. The trends observed for the evolution of the band center position and bandwidth with temperature may have several origins. In particular, the increase of the bandwidth may result from either a dynamical effects and/or due to the formation of hydrogen bonded species. On one hand, an increase of the temperature can activate the chemical exchange dynamics of the equilibrium H_2O+CO_2 ⇔ complex leading to band broadening of the Raman profile [20]. On the other hand, the strong increase of the concentration of water in the mixture should favoured water aggregates at the expense of the EDA CO_2-H_2O complex itself. However, we may argue as well that the reverse situation might be observed as increasing the temperature favours the breaking of water oligomers. In order to distinguish between these two hypotheses, we have performed further Raman experiments in the temperature range 40-340°C at P=250bar at constant water concentration (C_{H2O}=0.4 $Mol.dm^{-3}$). As the temperature is increased, a single narrow peak is observed, shifting continuously towards higher frequencies and its shape remains almost unchanged. The evolution of the band centre frequency and of the full width at half height of this profile has been calculated by fitting this profile with a Lorentzian line and is reported on Figure 5 (open square).

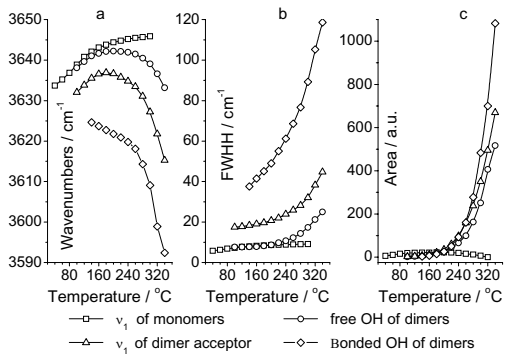

Fig. 5: Evolution of the fitted parameters as a function of the temperature for H_2O dissolved in the CO_2 phase: a) band center frequency, b) full width at half height (FWHH), c) integrated area.

Thus, the shift of the ν_1 mode towards higher frequencies might be attributed to a weakening of the strength of the CO_2-H_2O complex. Moreover, the FWHH of the ν_1 profile is found to be only slightly temperature dependent, suggesting that the strong increase of the width of the ν_1 mode

observed previously when the concentration of water increases in the mixture is related to water aggregates. To analyse the evolution of the band shape of the OH stretching mode as a function of the temperature and the concentration of water, we have decomposed the observed profiles using one Lorentzian for the band associated with the CO_2-H_2O EDA complex and one to three Gaussian profiles (depending on the temperature range) to represent the band associated with the water aggregates. Better fits were achieved using Gaussian profiles instead of Lorentzian ones indicating that an inhomogeneous distribution of water oligomers exist even at high temperature [21]. In the fitting procedure, we have fixed the width and the band centre frequency of the Lorentzian line associated with the CO_2-H_2O complex at the values obtained from the analysis of the profiles at constant water concentration. Using this procedure, a good fit of the data has been obtained and the values of the band centre frequency and the width of each profile are reported in Figure 5. We find that a single Lorentzian profile is sufficient to obtain a good fit of the data up to T=100°C. From this temperature and above, two additional Gaussian lines respectively centred at about 3638 and 3632 cm^{-1} are needed to obtain a good fit of the data in the temperature range 100-140°C. These profiles are slightly shifted to higher frequencies up to 3642 and 3636 cm^{-1} respectively as the temperature reaches 180°C. The values of the width of the profiles are about 9 and 18 cm^{-1} respectively and are almost constant in the temperature range 100-140°C. At temperatures greater than 140°C, a third Gaussian profile is needed to achieve a good fit of the data. From 140°C up to 340°C, the three Gaussian profiles centred respectively at 3638, 3632 and 3625 cm^{-1} are shifted to lower frequencies down to 3631, 3615 and 3592 cm^{-1} respectively and significantly broaden as the temperature reaches 340°C. Let's emphasise that, at temperatures greater than or equal to 320°C, three Gaussian profiles centred at 3600, 3620 and 3637 cm^{-1}, respectively, are sufficient to obtain good fit results without taking into account the contribution associated with the H_2O-CO_2 complex. This fact put in evidence the absence of solitary water in the system at highest temperatures.

4.3. Mid infrared absorption

The spectra measured in the OD stretching region of HDO in the CO_2 rich phase in the temperature range 40-340°C at constant pressure 250 bar are displayed on Figure 6. At 40°C, the spectrum has only one single well defined peak at about 2703 cm^{-1} which can be attributed to HDO monomers interacting with CO_2. Upon increasing temperature, the absorption intensity increases due to an increasing of water concentration in CO_2. However, in the temperature range 40-80°C, the band shape does not practically change and only a shift of the peak position towards higher frequencies accompanied by an increase of the width takes place. These findings indicate, that at T=80°C, water dissolved in the CO_2 phase still exists in its monomeric form. However, by further heating the fluid, a shoulder appears on the low wavenumber side of the peak centred at about 2655 cm^{-1}. Increasing again the temperature, this shoulder becomes a pronounced very broad peak. Because its frequency position is lower by about 52 cm^{-1} (at 100°C) and 65 cm^{-1} (at 300°C) from the monomeric one, we may assign the corresponding band to hydrogen-bonded aggregates of HDO.

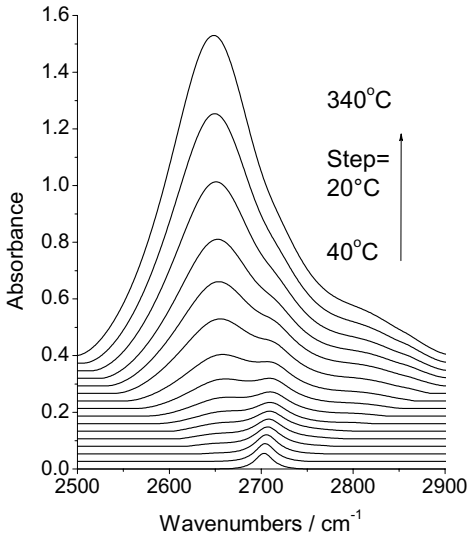

Fig 6: Infrared spectra of HDO in the CO_2 rich phase as a function of the temperature at constant pressure P=250 bar.

Due to the growth of this band, the absorption profile, which is constituted of a single line at low temperatures, becomes very broad and asymmetric at highest temperatures. Therefore, the increased absorption intensity of the low frequency band relatively to the one of monomer indicates that the ratio of the hydrogen bonded OD versus the

hydrogen-bond-free OD increases with the temperature. As discussed above in the Raman section, an increasing temperature has two opposite effects on the equilibrium between hydrogen-bonded and hydrogen-bond-free species. Heating the fluid increases the solubility of water in CO_2, leading to an increased concentration of hydrogen-bonded species. However, heating may also breaks oligomers favoring hydrogen-bond-free species which would be seen on the low frequency side of the profile assigned to monomeric water. To discriminate between these two possibilities, we have performed, as we did in Raman spectroscopy, infrared measurements at constant water concentration. The experimental spectra were fitted using Lorentzian profiles. From this comparison, we found that there is neither a strong shape modification of the experimental profile nor apparition of pronounced low frequency features. The fitted band centre frequency and FWHH associated with the monomeric profile are also reported on Figure 7. From their evolution with temperature, it is found that the band centre shifts continuously towards high frequencies and that the band width significantly increases. These results provide evidence that strong changes in the absorption band shape at increasing water concentration in the CO_2-rich phase are related to the formation of hydrogen-bonded species. To analyse the evolution

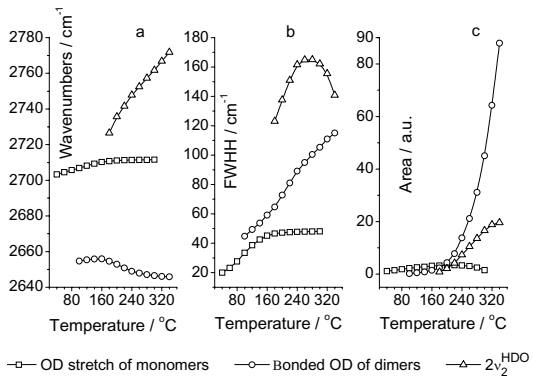

Fig. 7: Evolution of the fitted parameters as a function of the temperature for HDO dissolved in the CO_2 phase: a) band center frequency, b) full width at half height (FWHH), c) integrated area.

of the spectral shape of the OD stretching mode as a function of the temperature and the concentration of HDO in CO_2, we have applied the same type of decomposition of the profile that we did previously. We have decomposed the experimental profile into a single Lorentzian associated with monomeric HDO species and a Gaussian band for the hydrogen-bonded species. In the fitting procedure, the values of two parameters of the Lorentzian profile (namely the band centre frequency and the FWHH) have been fixed to those obtained from the analysis performed at constant water concentration. The fitted values are reported in Figure 7. It comes out from this comparison, that in the temperature range 40-100°C, a single Lorentzian profile is only needed to obtain a good fit of the spectra. In the temperature range 100 to180°C a Gaussian profile should be added. It is centred at about 2654 cm^{-1} and slightly shifts to higher frequencies, up to 2656 cm^{-1} as the temperature reaches 160°C, and then the band centre is noticeably displaced towards lower frequencies down to 2646 cm^{-1} at 340°C. At the same time, the width of this band strongly increases in the whole temperature range. It is noteworthy that at T=180°C and above, another Gaussian profile centred at about 2726 cm^{-1} should be added to improve the quality of the fit. This band can be assigned to the $2\nu_2$ overtone of the HDO bending mode. Upon increasing the temperature the peak position of this band shifts towards higher frequencies whereas its full width at half height increases achieving a maximum at 280°C. Finally, at temperature greater or equal to 320°C, two Gaussian profiles, centred at 2646 and 2770 cm^{-1} respectively, are enough to obtain a good fit. They are assigned to hydrogen-bonded species and to the $2\nu_2$ overtone of HDO respectively. Concurrently, the lack of the monomeric band indicates the absence of monomer species in the fluid at these temperatures.

5. Discussion

5.1. Assignment of the spectral components

In the previous section, the analysis of IR and Raman band shapes relies on the decomposition of the experimental curves into the minimum number of Lorentzian and Gaussian components. In order to assign these contributions, we have reported in Table 1 the characteristic frequencies of the monomer and H-bonded species (namely dimers and trimers) of HDO and H_2O which have been obtained from studies of water in the gas phase and in the low temperature Argon matrix.

Table 1. Assignment of the vibrational modes of water monomer (1), dimer (2) and trimer (3)

		Ar matrix	Gas phase	Present work	Assignment
H_2O	1		3756		ν_3
			3657	3634-3646	ν_1
	2	3726 (a)	3745 (c)		ν_3 acceptor
		3634 (a)	3600 (c)	3632-3615	ν_1 acceptor
		3709 (a)	3730 (c) 3735 (d)	3638-3633	donor free OH
		3574 (a)	3530 (c) 3601 (d)	3625-3592	donor OH-bonded
	3	3707 (a)	3726 (d)		free OH
		3516 (a)	3533 (d) 3532 (e)		OH-bonded
HDO	1	2710 (h)	2723 (f)	2703-2712	free OD
	2	2639 (h)	2658 (g)	2655-2646	OD-bonded
	3	2587 (b)	2575 (g)		OD-bonded

(a)[22], (b)[23] , (c)[24], (d)[25], (e)[26], (f)[27], (g)[28], (h)[29].

The comparison of these values with those of the band centres of the Lorentzian and Gaussian components obtained from the fits suggests that the profiles associated with the observed H-bonded species originates from dimeric species.

Indeed, for Raman spectra, the peak centred at about 3634 and 3646 cm^{-1} (at T=40 and 300°C respectively) which is well reproduced by a single Lorentzian profile was attributed to the ν_1 symmetric OH-stretching mode of monomeric water interacting with surrounding CO_2 molecules. The two Gaussian bands observed in the 3638-3615 cm^{-1} spectral domain (in the temperature range 100-340°C) can be assigned to the free OH of dimers and to the ν_1 symmetric stretching mode of the water acceptor molecule in the dimer (high and low frequency band respectively). The third broad Gaussian profile centred in the range 3624-3592 cm^{-1} (140-340°C) can be assigned to the stretching mode of the hydrogen-bonded OH group of dimers.

In IR absorption, the profile which is well reproduced by a single Lorentzian profile centred in the spectral domain 2703-2711 cm^{-1} in the temperature range 40 and 300°C was assigned to the OD-stretching mode of monomeric HDO. A single Gaussian band centered at 2655 and 2646 cm^{-1} (for 40 and 300°C respectively) was enough to nicely represent the hydrogen-bonded OD of dimers. Incidentally, it is interesting to point out that the widths of the Raman and IR profiles, associated with the OH group of hydrogen-bonded dimers strongly increase upon heating. For such inhomogeneously broadened spectra this finding may suggest that a larger distribution of OH bonded species is favored with the temperature.

Finally, it is noteworthy that characteristic vibrational frequencies of hydrogen bonded OD or OH groups of trimers are lower than the wavenumbers (see Table 1) of the spectral transition reported here. On the ground of this observation, we can infer that trimers and larger oligomers have likely a negligible concentration to be detected in the thermodynamic domain investigated here.

5.2. Determination of the concentration of the water species in CO_2

We found from our previous analysis that water monomers in the CO_2 phase only exist in the temperature range 40-80°C and therefore, under these conditions, the monomeric concentration $C_{H_2O}^{monomer}$ is equal to the total concentration C_{H_2O} of water.

In Raman spectroscopy, this allows to calculate a scattering activity coefficient $K_{monomer}^{*} = \left\langle A / C_{H_2O}^{monomer} \right\rangle$ from the integrated intensity A of the water vibrational transition and to use this value to determine the concentration of monomeric water above 80°C. Finally, the total dimer concentration is given as $C_{H_2O}^{dimer} = C_{H_2O} - C_{H_2O}^{monomer}$.

The calculated concentrations of the different water species are presented in Figure 8.

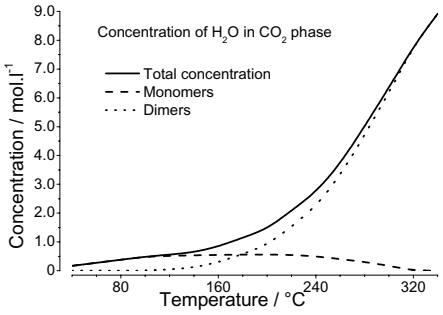

Fig 8: Concentration of H_2O species in the CO_2 rich phase as a function of the temperature calculated from Raman measurements (see text).

It appears clearly from this figure, that water dissolved in the CO_2 phase exists only under monomeric form and that its concentration noticeably increases upon heating in the temperature range 40-100°C. Dimers start to appear above 100°C with a marked increased

concentration with the temperature whereas the monomer concentration remains almost constant in the temperature range 120-220°C. A further heating of the fluid, leads to a strong decrease of the monomer concentration which vanishes above 300°C so that only H-bonded species are present in the CO_2 phase at this temperature.

In infrared spectroscopy, an isotopic mixture of H_2O and D_2O with ratios of 20:1 respectively has been used. The concentration C_{HDO} of HDO in the CO_2 phase is calculated from the reaction $H_2O+D_2O \xrightleftharpoons{K^{eq}} 2HDO$ using the value of the equilibrium constant K^0= 3.96 at 25°C reported in the literature [30]. At 25°C, C_{HDO} amount 10% of the total concentration of the water-mixture. The temperature dependence of the equilibrium constant follows the van't Hoff equation: dlnK/d(1/T)= -ΔH/R, in which ΔH, the enthalpy of the reaction, is equal to -12.7 J/mol [31].

Using the equilibrium constant obtained from the Arrhenius law and the known concentrations of H_2O and D_2O, the total concentration of HDO as a function of the temperature has been calculated as $C_{HDO} = \sqrt{K^{eq} \cdot C_{H_2O} \cdot C_{D_2O}}$ (see Figure 9).

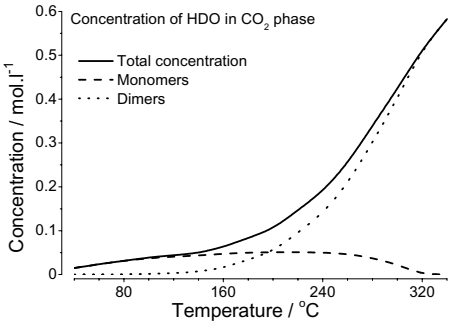

Fig 9: Concentration of HDO species in the CO_2 rich phase as a function of the temperature extracted from IR measurements (see text).

The determination of the concentration of HDO species (free and hydrogen-bonded) has been performed along the same approach used in Raman spectroscopy. In the temperature range 40-80°C the concentration of HDO monomeric species is equal to the total concentration of HDO in the CO_2 phase ($C_{HDO}^{monomer} = C_{HDO}$). Using this fact, the absorption coefficient $K_{monomer} = \left\langle A/(C_{HDO}^{monomer} \cdot l) \right\rangle$ (where l is the optical pathlength) was obtained and the concentration of monomeric HDO in the CO_2 phase at temperature above 80°C has been calculated. Concentrations of HDO monomers and dimeric species calculated as $C_{HDO}^{dimer} = C_{HDO} - C_{HDO}^{monomer}$ are presented in Figure 9. Although the concentration of HDO is ten times less than the concentration of H_2O dissolved in CO_2, the evolution of the quantity of monomers and dimers of HDO as a function of the temperature is in remarkable agreement with that reported in Raman.

6. Summary and Conclusions

In the present study, IR absorption and Raman scattering spectroscopies have been applied to investigate the evolution of the state of aggregation of water in the CO_2 rich phase as a function of temperature at constant pressure P=250 bar. The analysis of band shape variations led us to conclude, that below 100°C water exists only in its monomeric form, whereas H-bonded species, namely dimers, start to appear at higher temperature. Upon heating, the dimer concentration increases at the expense of the monomer one such that only dimers are detected in CO_2 at the temperature close to that of total miscibility of the mixture. It is noteworthy that the results obtained so far using Raman and IR spectroscopy complement nicely each others and lead to a consistent view of the structural organization of water in the mixture.

Acknowledgements

Roman Oparin is pleased to thank the Ministère de la Recherche for a postdoctoral fellowship under the auspices of which this work has been completed.

The authors would like to thank Regis Thiéry from the University of Clermont-Ferrand for providing the density values of the CO_2 rich phase using an equation of state of Daridon et al [5].

References and Notes

[1] F. Cansell, C. Aymonier, and P. Beslin, *Environ. Prog.* **17**, 258 (1998); P. E. Savage, *Chem. Rev.* **99**, 603 (1999).

[2] K. Todheide and E. U. Franck, *Z. Phys. Chem. Neue Folge* **37**, 387 (1963).

[3] A. E. Mather and E. U. Franck, *J. Phys. Chem.* **96**, 6 (1992); M. B. King, A. Mubarak, J. D. Kim, and T. R. Bott, *J. Supercritical Fluids* **5**, 296 (1992); S. Takenouchi and G. C. Kennedy, *Am. J. Sci.* **262**, 1055 (1964); J. S. Gallagher, R. Crovetto, and J. M.

H. Levelt-Sengers, *J. Phys. Chem. Ref. Data* **22**, 431 (1993).
[4] Z. Duan, N. Moller, and J. H. Weare, *Geochim. Cosmochim. Acta* **56**, 2619 (1992); R. J. Bakker, *Chemical Geology* **194**, 3 (2003).
[5] J. L. Daridon, *PhD Thesis Université de Pau et des Pays de l'Adour*, 177 (1992); J. L. Daridon, H. Lagourette, H. Saint-Guirons, and P. Xans, *Fluid Phase Equilibria* **91**, 31 (1993).
[6] E. L. Shock, (Kluwer Academic Publishers, 1992), Vol. 22, pp. 67; M.-P. Bassez, *J. Phys. Condens. Matter* **15**, 353 (2003).
[7] A. L. Narvor, E. Gentric, and P. Saumagne, *Can. J. Chem.,* **49**, 1933 (1971).
[8] M. J. Clarke, K. L. Harrison, K. P. Johnston, and S. M. Howdle, *J. Am. Chem. Soc.* **119**, 6399 (1997).
[9] L. E. Bowman, B. J. Palmer, B. C. Garett, J. L. Fulton, C. R. Yonker, D. M. Pfund, and S. L. Wallen, *J. Phys. Chem.* **100**, 18327 (1996).
[10] A. J. Cox, T. A. Ford, and L. Glasser, *J. Mol. Struct.* **312**, 101 (1994).
[11] N. R. Zhang and D. D. Shillady, *J. Chem. Phys.* **100**, 5230 (1994); Y. Danten, T. Tassaing, and M. Besnard, *J. Phys. Chem. A*, in press (2004).
[12] Y. Danten, T. Tassaing, and M. Besnard, *J. Mol. Liq.*, in press (2004).
[13] T. Tassaing, R. Oparin, Y. Danten, and M. Besnard, *J. Supercritical Fluids* **in press** (2004).
[14] X. Bin, K. Nagashima, J. M. Desimone, and C. S. Johnson, *J. Phys. Chem. A,* **107**, 1 (2003).
[15] S. Rey, PhD thesis, Bordeaux I, 1999.
[16] G. Herzberg, in *Molecular Spectra and Molecular Structure: Infrared and Raman Spectra of Polyatomic Molecules* (D. Van Nostrand Company, Inc., Princeton, New Jersey, 1956), Vol. II, pp. 273.
[17] H. G. Kjaergaard, B. R. Henry, H. Wei, S. Lefebvre, T. Carrington, O. S. Mortensen, and M. L. Sage, *J. Chem. Phys.* **100**, 6228 (1994).
[18] G. R. Low and H. G. Kjaergaard, *J. Chem. Phys.* **110**, 9104 (1999).
[19] R. Knochenmuss and S. Leutwyler, *J. Chem. Phys.* **96**, 5233 (1992).
[20] M. I. Cabaco, M. Besnard, and J. Yarwood, *Mol. Phys.* **75**, 157 (1992).
[21] D. M. Carey and G. M. Korenowski, *J. Chem. Phys.* **108**, 2669 (1998); S. Furutaka and S. Ikawa, *J. Chem. Phys.* **113**, 1942 (2000).
[22] R. M. Bentwood, A. J. Barnes, and W. J. O. Thomas, *J. Mol. Spectrosc.* **84**, 391 (1980).
[23] A. Engdahl and B. Nelander, *J. Chem. Phys.* **86**, 4831 (1987).
[24] Z. S. Huang and R. E. Miller, **91**, 6613 (1989).
[25] F. Huisken, M. Kaloudis, and A. Kulcke, *J. Chem. Phys.* **104**, 17 (1996).
[26] J. B. Paul, C. P. Collier, R. J. Saykally, J. J. Scherer, and A.O'Keefe, *J. Phys. Chem. A,* **101**, 5211 (1997).
[27] N. Papineau, C. Camy-Peyret, J.-M. Fraud, and G. Guelachvili, *J. Mol. Spectrosc.* **92**, 451 (1982).
[28] J. G. van Duijneveldt-van de Rijdt and F. B. van Duijneveldt, *Chem. Phys* **175**, 271 (1993).
[29] G. P. Ayers and A. D. E. Pullin, *Spectrochim. Acta A* **32A**, 1629 (1976).
[30] F. O. Libnau, A. A. Christy, and O. M. Kvalheim, *Applied Spectroscopy* **49**, 1431 (1995).
[31] A. Narten, *J. Chem. Phys.* **41**, 1318 (1964).